J Mater Sci: Mater Med (2011) 22:2413–2427
DOI 10.1007/s10856-011-4435-z

Hydroxyapatite nanorod-reinforced biodegradable poly(L-lactic acid) composites for bone plate applications

Erkin Aydin · Josep A. Planell · Vasif Hasirci

Received: 7 March 2011 / Accepted: 25 August 2011 / Published online: 15 September 2011
© Springer Science+Business Media, LLC 2011

Abstract Novel PLLA composite fibers containing hydroxyapatite (HAp) nanorods with or without surface lactic acid grafting were produced by extrusion for use as reinforcements in PLLA-based bone plates. Fibers containing 0–50% (w/w) HAp nanorods, aligned parallel to fiber axis, were extruded. Lactic acid surface grafting of HAp nanorods (lacHAp) improved the tensile properties of composites fibers better than the non-grafted ones (nHAp). Best tensile modulus values of 2.59, 2.49, and 4.12 GPa were obtained for loadings (w/w) with 30% lacHAp, 10% nHAp, and 50% amorphous HAp nanoparticles, respectively. Bone plates reinforced with parallel rows of these composite fibers were molded by melt pressing. The best compressive properties for plates were obtained with nHAp reinforcement (1.31 GPa Young's Modulus, 110.3 MPa compressive strength). In vitro testing with osteoblasts showed good cellular attachment and spreading on composite fibers. In situ degradation tests revealed faster degradation rates with increasing HAp content. To our knowledge, this is the first study containing calcium phosphate–polymer nanocomposite fibers for reinforcement of a biodegradable bone plate or other such implants and this biomimetic design was concluded to have potential for production of polymer-based biodegradable bone plates even for load bearing applications.

E. Aydin · V. Hasirci
BIOMATEN, METU Center of Excellence in Biomaterials and Tissue Engineering, Ankara, Turkey
e-mail: erkin.aydin.1@gmail.com

E. Aydin · V. Hasirci
Department of Biotechnology, Biotechnology Research Unit, METU, 06800 Ankara, Turkey

J. A. Planell
Institute for Bioengineering of Catalonia (IBEC), C/Baldiri i Reixach, 4–6, Tower I, 10th floor, 08028 Barcelona, Spain
e-mail: japlanell@ibecbarcelona.eu

V. Hasirci (✉)
Department of Biological Sciences, Biotechnology Research Unit, METU, 06800 Ankara, Turkey
e-mail: vhasirci@metu.edu.tr

1 Introduction

Diaphyseal fractures are common fracture patterns of the long bones, and the usual strategy in their treatment is to use bone plates to restrain the movement of the fragments. In such an application, the bone plate carries the compressive load applied to the bone fragments throughout the healing process (around 1–1.5 years). The conventional compression plates are made of metals, including stainless steel and titanium as well as alloys such as cobalt-chromium [1–3]. Elastic modulus of human cortical bone is in the range 15–26 GPa, however, that of metals are 5–10 times higher [4]. This modulus mismatch leads to stress-shielding effect, the result of which is decrease of the bone mineral mass leading occasionally to bone fracture after the plate removal. Stress shielding is caused by the absence of load on the healing bone because of the metal plate taking over all the stress transfer. Another problem with the use of metal plates is corrosion and/or accumulation of metallic particles in the vicinity of the implant that may alter osteoblast behavior even at subtoxic levels [5], or at distant body parts including draining lymph nodes, spleen and liver [6]. Finally, a metal bone plate has to be removed by surgery after healing is accomplished.

To avoid the stress-shielding, it is desirable to use plates made of materials with mechanical properties close to those of the bone. The best candidates are polymers,

especially the biodegradable ones that would not cause long term foreign particle accumulation in the body and would eliminate the cost and discomfort of a removal surgery. Therefore, studies on such biodegradable polymeric osteofixation devices have been continuing since the introduction of first biodegradable devices in 1966 [7]. Poly(L-lactide) (PLLA) is one of the sturdiest and most frequently adopted biodegradable polymer in bone fixation systems [8–11], however, the most prevalent problem reported about those devices is their mechanical properties that cannot approximate to those of bone.

The inherently better mechanical properties of PLLA among other polylactides is due to its semicrystalline structure, where the steric effects cause tight association in crystallite regions which act like crosslinks between polymer chains and improve the mechanical properties. The crystallite regions, though, are not degraded as fast as the polymer backbone and mobilized and released into circulation. Although these free particles were reported to have a risk to evoke a highly inflammatory body response against PLLA in some cases [12], lack of sufficient sources of alternative biodegradable polymers with comparable mechanical properties and generally accepted high biocompatibility of polylactide polymers are the reasons for the never-ending interest for PLLA in mechanically demanding applications.

Although the mechanical demand on metallic and ceramic biomaterials is normally below their ultimate strengths, these requirements are generally higher than the capability of polymers, making them prone to mechanical failure [13]. At this point, polymer composites appear as potential candidates in overcoming this mechanical disadvantage [14–16]. Composites of biodegradable polymers with hydroxyapatite (HAp) are especially attractive for bone tissue applications because calcium phosphate–polymer composites create a highly biocompatible [17] and osteoconductive product [18–21]. HAp can also tightly bind to the bony tissue chemically so that the bone and implant unite [22, 23]. Furthermore, the sustained release of calcium and phosphate from those composites is an added benefit, where the two ions serve as substrates in remodeling reactions of mineralized tissues [24].

The nano-scaled crystal structure of natural apatite explains the reason behind the superior mechanical properties of bone over any biomaterial designed for use in long bone healing [25]. In this study, HAp nanorods were used to mimic the natural apatite of the bone. In order to increase the mechanical strength, HAp nanorods were aligned parallel both to the composite fibers and the long axis of the bone plate, a design that occurs in long bones where collagen fibers with distributed nano apatite crystals are aligned parallel to the long axis of bone.

In the literature, there are quite a number of examples for use of micro or nano HAp rods/fibers or particles in composite biodegradable polymeric biomaterials designated for use in bone fixation or grafting [26–32]. Despite different sample geometries which were tested for different aspects including tensile, compressive, or bending usually resulted in non-comparable results, it can be deduced that all these composites resulted in superior mechanical properties for bone repair applications than their monophasic counterparts. Studies with continuous fiber reinforced biodegradable plates are also available, in a lower number of cases, in the literature [33, 34]. Composites containing newly developed reinforcements of continuous or short phosphate glass fibers with 10–20 μm diameters were also suggested as alternatives for HAp fibers with claims of high mechanical properties and complete biodegradation [35, 36]. However, to our knowledge, this is the first study in the literature where calcium phosphate–polymer nanocomposite fibers are used in the reinforcement of a biodegradable bone plate or any other implant. Furthermore, loaded calcium phosphate particles were in the form of nanorods and the here presented technique enabled their placement parallel to the long axis of the implant, mimicking the bone's microscopic structure with the expectation that this design also attains the mechanical properties of the implant.

Use of continuous reinforcing fibers is a common practice in manmade composite materials adopted for increased mechanical properties towards the fiber alignment direction. In the structure of bones, however, nature utilized non-continuous but still aligned slender apatite nanoparticles for reinforcement of the collagen fibers, the main matrix component. This discrete pattern was suggested to provide bones enough strength and toughness without being brittle due to the elimination of crack propagation throughout the reinforcement axis [25]. This design pattern was mimicked in the current study with the hypothesis that it can help increase mechanical properties of PLLA as bone plates or other devices for fixation of load bearing bones in a completely biodegradable manner.

HAp nanorods with 50–150 nm length with 5–20 nm diameters were hydrothermally synthesized. They were then surface grafted with lactic acid in order to achieve both a higher chemical compatibility between HAp nanorods and the PLLA matrix and to have a more homogenous distribution of nanorods within the polymer. Nanocomposite fibers of PLLA and HAp nanorods were prepared by extrusion and tensile tested. The bone plates were produced by embedding these composite fibers within PLLA matrix in a mold via melt pressing and the plates were mechanically tested for compression. In situ degradation studies in PBS and in ultrapure water were carried out and weight loss and pH change were followed for up to 6 weeks. In vitro studies were done using rat bone marrow stem cells to study the interaction of nanocomposite fibers with osteoblasts.

2 Materials and methods

2.1 Materials

Poly(L-lactide) (Resomer L210, i.v. 3.3–4.3 dl/g) was purchased from Boehringer-Ingelheim (Germany). Lactic acid (90%), and hydroxyapatite (amorphous nano-micro particles, cHAp) were obtained from Fluka (Switzerland). Dexamethasone, β-glycerophosphate disodium salt, and glutaraldehyde solution (grade I, 25%) were purchased from Sigma-Aldrich (Germany). Dulbecco's Modified Eagle Medium (DMEM, high glucose) and fetal bovine serum were obtained from Hyclone (USA). Alamar Blue cell proliferation assay was from Invitrogen (USA). FITC-phalloidin and DAPI were obtained from Sigma (USA).

2.2 Synthesis of hydroxyapatite nanorods

Hydroxyapatite (HAp) nanorods were synthesized by modifying the method reported by Yubao et al. [37]. Briefly, 0.3 M $(NH_4)_2HPO_4$ and 0.5 M $Ca(NO_3)_2$ aqueous solutions were prepared, pH was adjusted to 11 with ammonia solution and the phosphate solution was added at a constant rate into the calcium solution while stirring. The suspension was heated at 70°C for 2 h, washed with distilled water, ethanol, and acetone, and then heated at 140°C for 2 h, washed with distilled water and the precipitate was dried under vacuum.

2.3 Lactic acid surface grafting of HAp nanorods

The synthesized HAp nanorods were surface grafted with lactic acid according to procedure of Qiu et al. [38]. In brief, the nanorods (1 g) and lactic acid solution (1.2 or 2.2 g) were heated in a flask containing 30 ml tetrahydrofuran (THF) and 45 ml toluene at 150°C for 10 h. Then, the particles were washed with THF and ethyl acetate and dried. FTIR spectrometry was carried out with a Jasco 4200 (Japan) spectrometer. Elemental analysis of the lacHAp and nHAp for carbon and hydrogen were carried out in a CHNS-932 elemental analysis system (LECO, USA).

2.4 Preparation of nanocomposite fibers

Predetermined amounts of hydroxyapatite (nHAp, lacHAp, cHAp) were suspended in 5 ml chloroform using a probe ultrasonicator (Cole-Palmer Instruments, 4710 series, USA) at 25 W for 2 min and then added into a PLLA in chloroform solution (5%, w/v) to obtain a HAp fraction of 0, 10, 20, 30, 40, or 50% (w/w) (total mass of HAp and PLLA is 2 g). The PLLA solution was further incubated in a Branson 2200 ultrasonic bath (Branson Co., USA) at 60 W for 6 h. The content was poured in a petri plate, dried in air overnight, cut into about 0.5 cm × 0.5 cm chips and further dried under vacuum at 50°C for 8 h. The chips were extruded with a Dynisco LCR 7001 capillary rheometer (Roper industries Inc., USA) at different temperatures (165–225°C) and the products were collected as continuous fibers. To be used in in vitro evaluations, some of the fibers were aligned side by side and attached to each other by spraying with chloroform and air drying so that they provide cells ca. 1 cm × 1 cm attachment surface.

2.5 Production of bone plates

In order to evaluate the reinforcing effect of composite fibers on the bone plates, one or two layers of fibers (each layer containing 8 individual 5 cm-long composite fibers that were parallel to each other and longitudinally placed) were buried within a PLLA matrix in a custom designed mold (5 cm × 1 cm × 0.3 cm). The particular mold was determined to accommodate an amount of 2 g PLLA powder to obtain the best result in plate production. Therefore, the amount of PLLA powder to be put into the mold, along with reinforcing composite fibers, was determined by subtracting the total weight of reinforcing fibers from 2 g. The obtained amount was divided equally into two or three for producing plates reinforced with one or two layers of composite fibers, respectively. In the case of one layer of fiber reinforcement, one portion PLLA powder was spread on the bottom of mold, a layer of 8 reinforcing fibers was placed over powder and the other portion of PLLA powder was poured on top (total fibers/plate volume fraction is 0.12). In the case of two reinforcing layers (each having 8 fibers), an arrangement of the PLLA powder portions were placed in the same fashion but this time two layers of fibers were sandwiched within the structure so that there is another PLLA powder layer between these fiber layers (volume fraction is 0.24). A maximum of 8 fibers could be placed in each layer so that they will be parallel to the plate's c-axis, be completely buried within the plate matrix and do not touch or intersect each other. After filling the materials, upper part of the mold, which can tightly fit into the inner compartment, was placed. The mold was heated to 175°C and 2 bar pressure was applied for 1 h while keeping the same temperature. Then the heater was stopped and pressure was relieved after the mold cooled to room temperature.

2.6 Scanning electron microscopy

SEM and STEM (Scanning Transmission Electron Microscopy) investigations of the nanorods were done after air drying ethanol dispersion on a SEM stub. Internal structures of the composite fibers were investigated after exposing the cross section with freeze fracture. Quanta

400F model field emission SEM (FEI Co., USA) was used in the visualizations.

2.7 Mechanical testing

The tensile properties of 5 cm long PLLA–HAp composite fibers were determined under the conditions defined in ASTM D638-08 with 2 cm gage length and 1.2 cm/s crosshead speed using MT-LQ model mechanical tester (Stable Micro Systems, UK) with a 2500 N load cell. Tensile tests were repeated at least for 5 times.

For compression testing of the plates (25 mm × 10 mm × 3 mm) through their long axes, ASTM D695-08 was followed and a support jig was used as advised. The tests were performed at a crosshead speed of 1.3 cm/min using Lloyd LRX5 K tester with a 5000 N load cell (Lloyd Instruments Limited, UK). All the compressive tests were repeated twice.

2.8 In situ degradation studies

Composite fibers were tested for degradation according to the directives of ASTM F1635-04a. After bringing the composite fibers to a constant weight, fibers were cut to be between 1.5 and 2 cm lengths (depending on fiber diameter) so that each fiber weighed ca. 60 mg. They were maintained within capped test tubes containing phosphate buffered saline (PBS, 10 ml, 0.1 M, pH 7.4) for up to 6 weeks on an orbital shaker (37°C, 50 rpm). At predetermined time points, the fibers were removed, gently washed with distilled water, dried in vacuum oven until constant weight and the weights were recorded.

The same test was repeated with ultrapure water in order to determine pH changes. At the end of each time interval, pHs of the solutions were recorded with Eutech Cyberscan pH510 (Thermo Fisher Scientific, USA). All degradation and pH change tests were studied in triplicates and results were averaged.

2.9 In vitro behavior of composite fibers

2.9.1 Cell culture studies

The interaction between the composite fibers and rat bone marrow stem cells were evaluated by determining cell proliferation and spreading. Isolation of mesenchymal osteoprogenitor cells from femurs and tibiae of 6 week old male Sprague-Dawley rats was done according to Kose et al. [39]. After reaching confluency, isolated cells were lifted by 0.05% trypsin-EDTA and resuspended in osteogenic medium (DMEM with 20% fetal bovine serum, 100 units/ml penicillin, 100 μg/ml streptomycin, 1 μg/ml amphotericin B with 10 mm β-glycerophosphate, 50 μg/ml L-ascorbic acid and 10 nm dexamethasone). Cell suspensions (2.5×10^5 cells in 50 μl) were seeded on ethanol sterilized PLLA-HAp composite fiber constructs (1 cm × 1 cm) that were placed in 6-well plates. After waiting for an initial attachment for 30 min, more medium was added to cover the samples. The cells were grown for up to 2 weeks and media were refreshed every other day. Number of viable cells was assessed using Alamar Blue assay according to the procedure supplied by manufacturer. The test media in the wells were then discarded, washed with sterile PBS, fresh medium was added to the wells and the incubation was continued. Each sample was studied in triplicates and Alamar Blue assay was studied in duplicates for each triplicates and averaged. Statistical significance was determined by unpaired, two-tailed Student's *t*-test at a 95% confidence interval.

2.9.2 Confocal laser scanning microscopy

In order to study cell morphologies, cell–seeded composite fiber constructs were incubated for 3 days, rinsed with PBS and fixed with 4% p-formaldehyde in PBS for 30 min at room temperature. The samples were then treated with Triton X-100 (0.1%) for 5 min, washed with PBS, and incubated at 37°C for 30 min in BSA-PBS (1%) solution. Then the plates were stained with 1:100 diluted FITC-labeled phalloidin for 1 h at 37°C to stain actin filaments. After several washes with PBS, samples were treated with 1/3000 diluted DAPI for 4 min at room temperature to stain the nuclei. Afterwards, the samples were washed with PBS and studied with the confocal laser scanning microscope (TCS SPE, Leica, Germany) with a 488 nm laser for FITC-phalloidin and 358 nm light for DAPI. The images obtained at both wavelengths were overlaid.

2.9.3 Electron microscopy

Cell-seeded composite fiber constructs were washed with PBS and then with 0.1 M cacodylate buffer (pH 7.4), incubated in 2.5% glutaraldehyde solution for 2 h at room temperature, washed with cacodylate buffer and dried under vacuum. They were then coated with gold–palladium sputtering and examined with FEI Nova NanoSEM 430 model SEM (FEI, USA). Energy dispersive X-ray spectroscopy (EDX) was also conducted with the same system.

3 Results and discussion

3.1 Production of PLLA–HAp nanocomposites

The hydrothermal synthesis resulted in nanorods of 50–150 nm length with 5–20 nm diameters (Fig. 1). EDX

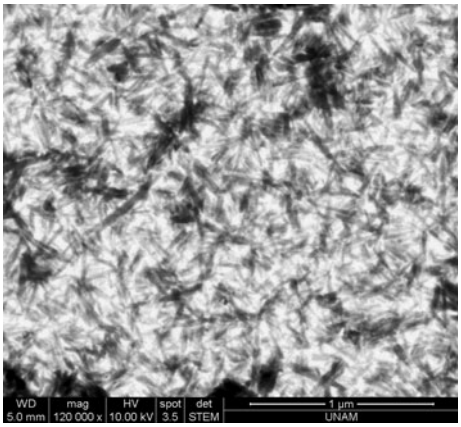

Fig. 1 Scanning-transmission electron microscope image of hydrothermally synthesized HAp nanorods

analysis revealed that they were calcium deficient hydroxyapatite with a Ca/P of 1.56, which is lower than that of HAp (1.67). This indicates that these nanorods will dissolve faster than HAp does and is very suitable for a biodegradable bone plate application.

The obtained HAp nanorods were chemically grafted with lactic acid, the monomer of the fiber and plate matrix (PLLA), with the hypothesis that lactic acid graft on the surface of HAp nanoparticles will increase compatibility with the surrounding PLLA matrix and help a more strongly association to the matrix. A high degree of interface strength could also be attained, for example, using an in situ polymerization technique, however, alignment of the HAp nanorods through fiber and plate c-axis would not be possible in such a case.

3.2 FTIR analysis of lactic acid–surface grafted HAp nanorods

Figure 2 shows the IR analysis results of lactic acid grafted HAp (lacHAp) and of pure HAp and lactic acid. The products' IR spectra resemble very much that of calcium phosphate which is expected because the bulk of the composite is calcium phosphate. There is very little indication of lactic acid binding. The 1583 and 1418 cm^{-1} peaks are not present in the spectra of either nHAp or lactic acid, and are attributed to $\nu_{as}COO^-$ and $\nu_s COO^-$ vibrations, respectively, of lactate species in calcium lactate [40], which apparently formed as a result of grafting.

3.3 Elemental analysis of HAp nanorods

Lactic acid surface grafting was confirmed more distinctly by the elemental analysis data for nHAp and lacHAp samples. When grafting was carried out using a lactic acid to HAp ratio of 1.2 or 2.2, the C and H contents were found to be 2.12 and 0.78%, respectively, in both cases. The proposed mechanism for grafting of lactic acid onto HAp involves loss of –OH from HAp, loss of –H from lactic acid and ionic association of Ca and lactic acid, releasing a H_2O molecule per bond (Eq. 1) [38]. Although there are 5 calcium atoms in each nHAp molecule, there is only one hydroxyl group; therefore, association of only one lactic acid is possible with each nHAp molecule. Since the only carbon source in lacHAp is lactic acid, 2.12% (w/w) carbon content indicates that a fraction of lactic acid (5.24%, w/w) is present in lacHAp. Theoretically, in order to have 1 lactic acid to be bound to 1 HAp molecule, the weight fraction of lactic acid in lacHAp must be 15.5% (w/w). So our result indicates that the lactic acid grafting efficiency is ca. 34%, or in other words, one in every three nHAp has a lactic acid bound to it. Since the tests started with 1.2:1 or 2.2:1 (w/w) nHAp to lactic acid ratio in preparation solutions led to the same result, 34% appears to be the maximum grafting efficiency that could be obtained under these reaction conditions.

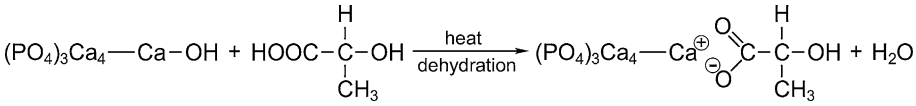

1

3.4 Production of nanocomposite fibers

Nanocomposite fibers produced with capillary rheometer had smooth surfaces, with no cracks or air bubbles all along the fiber length. Fiber diameters were between 0.60 mm and 0.94 mm, depending on the HAp content and the process temperature. Cross-section and the surface of pure PLLA fibers were also very smooth without air bubbles or cracks (Fig. 3a, b). On the other hand, the surface of the 40% (w/w) cHAp containing composite fibers were very rough with large numbers of small and large voids both on the outer surface and the cross-section (Fig. 3c, d). The cHAp particles were more or less evenly distributed within the polymer bulk (Fig. 3d). The outer fiber surface and the cross-section of the 40% (w/w) nHAp containing composite fibers were much smoother than the cHAp

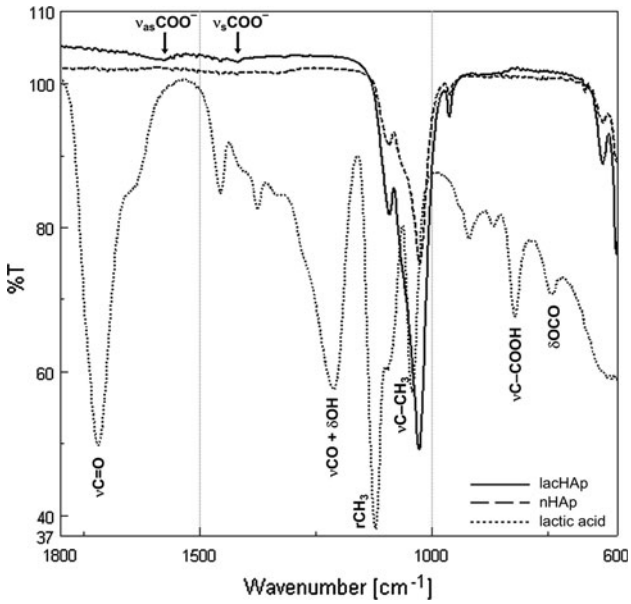

Fig. 2 FTIR-ATR spectra of lacHAp, nHAp and lactic acid. *Arrows* indicate the 1583 and 1418 cm^{-1} bands attributed to $\nu_{as}COO^{-}$ and $\nu_{s}COO^{-}$ vibrations in lactate ion, respectively (as: asymmetric, s: symmetric). Other peaks belong to the lactic acid groups

containing composites (Fig. 3e, f). There were no voids in the cross-section but very small voids, in both number and size, were observed on the outer fiber surface. nHAp particles were very evenly distributed within the polymer bulk and a detailed examination of the Fig. 3f reveals that most of the nHAp lay parallel to the fibers (extrusion axis or the z axis). The alignment was also evident in the SEM images of longitudinal sections from nHAp–PLLA fibers (Fig. 3g, h). This type of orientation of the nanorods can be explained by the fact that the large shear force, which is parallel to the flow axis of the molten polymer, acts on the freely moving HAp nanorods to force them to move parallel to the direction of motion and make their long axis almost parallel to the flow axis. Since there are no such strong forces acting on the polymer melt in x or y axis directions, long axis of the HAp nanorods could deviate from the flow axis. This type of inclinations of the nanorods could be eliminated by creating simultaneous forces directed towards the center of the rod. Therefore, it is evident from these observations that HAp nanorods within PLLA matrix can be aligned parallel to the extrusion axis of composite fibers produced with capillary rheometer. Additionally, a die having a conical flow path with a continuously decreasing barrel diameter could provide a better alignment of the nanorods.

The lacHAp particles in the 40% (w/w) lacHAp–PLLA composites fibers (Fig. 3j) have a high degree of aggregation, causing a non-homogenous distribution and no signs of alignment within the polymer bulk. On the other hand, distribution of lacHAp particles in the 10% (w/w) lacHAp–PLLA composite fibers revealed a better distribution pattern in the polymer and an alignment along the extrusion axis, just like the nHAp particles (Fig. 3j, insert). Therefore, lactic acid grafting of HAp particles seem to favor self-aggregation, instead of associating with the PLLA, and prevent even distribution of the HAp particle within the composites loaded with high amounts of HAp.

3.5 Tensile properties of composite fibers

HAp particles are much stiffer than the polymer and they are not ductile because of the crystalline structure. This high stiffness can influence the tensile properties of the resulting composite fiber only when the polymer and HAp particles have some sort of interaction. The nHAp loaded fibers showed their best performance at 10% loading by increasing the Young's Modulus (YM) values over that of unloaded fibers (Fig. 4), while 20% and 30% loadings caused similar YM values with the unloaded ones. The composite fibers containing 40 and 50% nHAp were so brittle that it was not possible to test them.

Increasing the lacHAp nanorod content, up to 30% of the composite, increased the YM values, after that the YM starts to decrease but reached a YM value lower than that of unloaded fibers at a loading as high as 50% (Fig. 4). The decrease in the mechanical properties of 40 and 50% lacHAp containing fibers is probably the result of high level of agglomeration of the nanorods within the polymer matrix which was not observed in lower levels of lacHAp loadings (data not shown). Nevertheless, lactic acid grafting improved the tensile properties significantly, especially at higher HAp loadings, as also was observed by Hong et al. [41]. The Ultimate Tensile Strength (UTS) values decreased with all three HAp species and at any loading ratio (Fig. 5) but the decrease in nHAp containing fibers was sharper, compared with the case of lacHAp containing ones. With essentially the same geometry and size of lacHAp and nHAp particles in mind, these observations suggest that surface grafting HAp nanorods with lactic acid is effective in improving the interfacial strength between the filler and the matrix and thus the tensile properties over those of nongrafted nanorods.

Surprisingly, the composite fibers loaded with the commercial HAp source (cHAp) showed the best tensile YM and UTS values at all compositions. One possible explanation to this observation might be that because the amorphous HAp particles were rough and irregular, they can mechanically interlock the polymer molecules in the bulk and thus improve the tensile properties, as suggested by Cheang and Khor [42]. Surface area of the individual cHAp particles is also much higher due to their irregular surface topologies. These two phenomena are not observed with nanofibrous rod-type fillers with smooth surfaces used

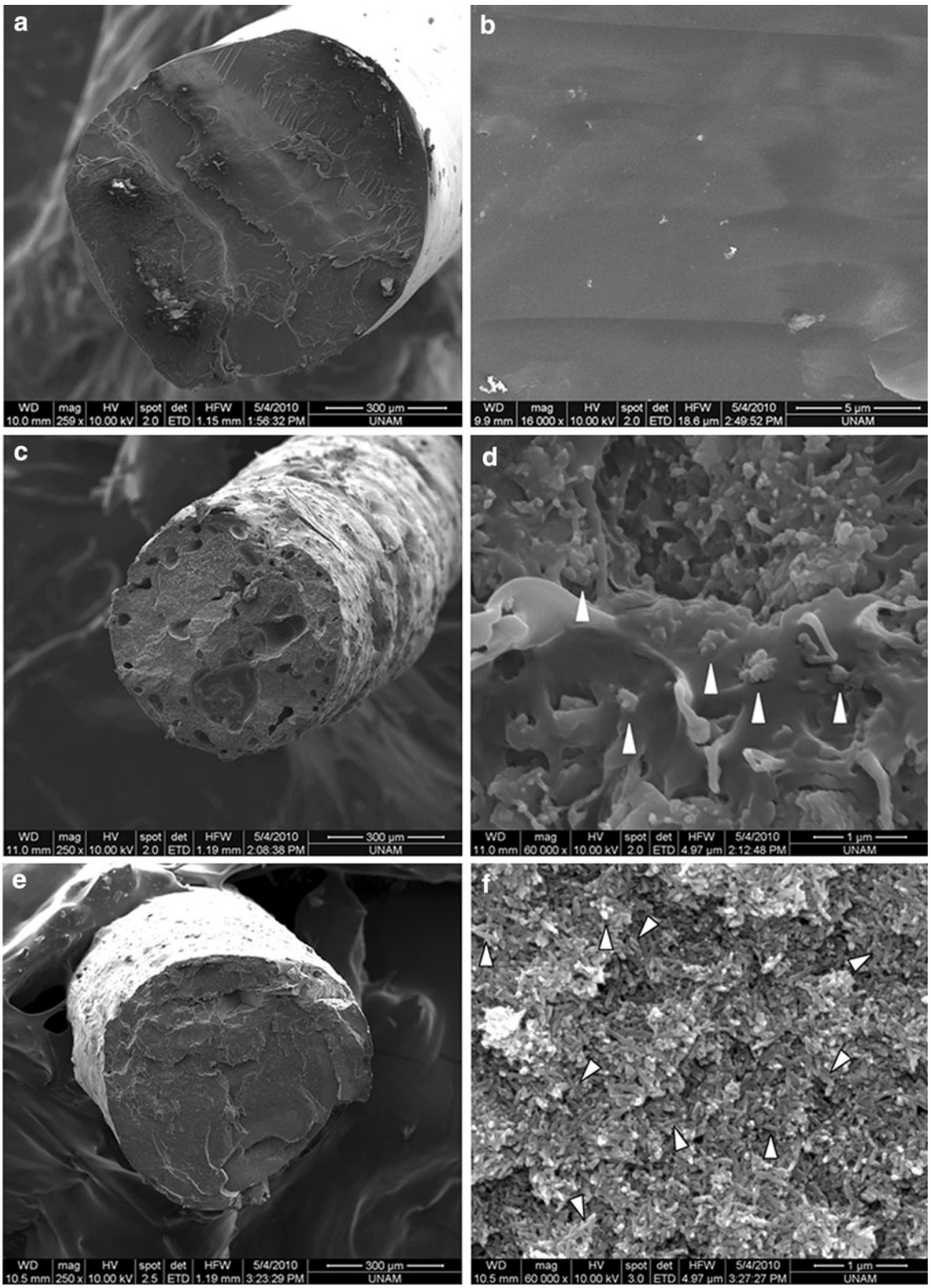

Fig. 3 SEM micrographs of freeze fractured pure PLLA or HAp–PLLA composite fibers. Cross sectional view of pure PLLA fibers: (**a**) ×259, (**b**) ×16,000. Cross sectional view of 40% cHAp–PLLA fibers: (**c**) ×250, (**d**) ×60,000 (*arrowheads*: cHAp particles). Cross sectional view of 40% nHAp–PLLA fibers: (**e**) ×250, (**f**) ×60,000 (*arrowheads*: some of the nHAp particles). Longitudinal section view of 40% nHAp–PLLA fibers: (**g**) ×150 (*arrow*: flow direction), (**h**) ×50,000 (*inset*: ×100,000, arrowheads: some of the nHAp particles). Cross sectional view of 40% lacHAp–PLLA fibers: (**i**) ×250, (**j**) ×30,000 (*arrowheads*: aggregates of lacHAp particles; *inset*: 10% lacHAp–PLLA, ×100,000, cross-sectional view)

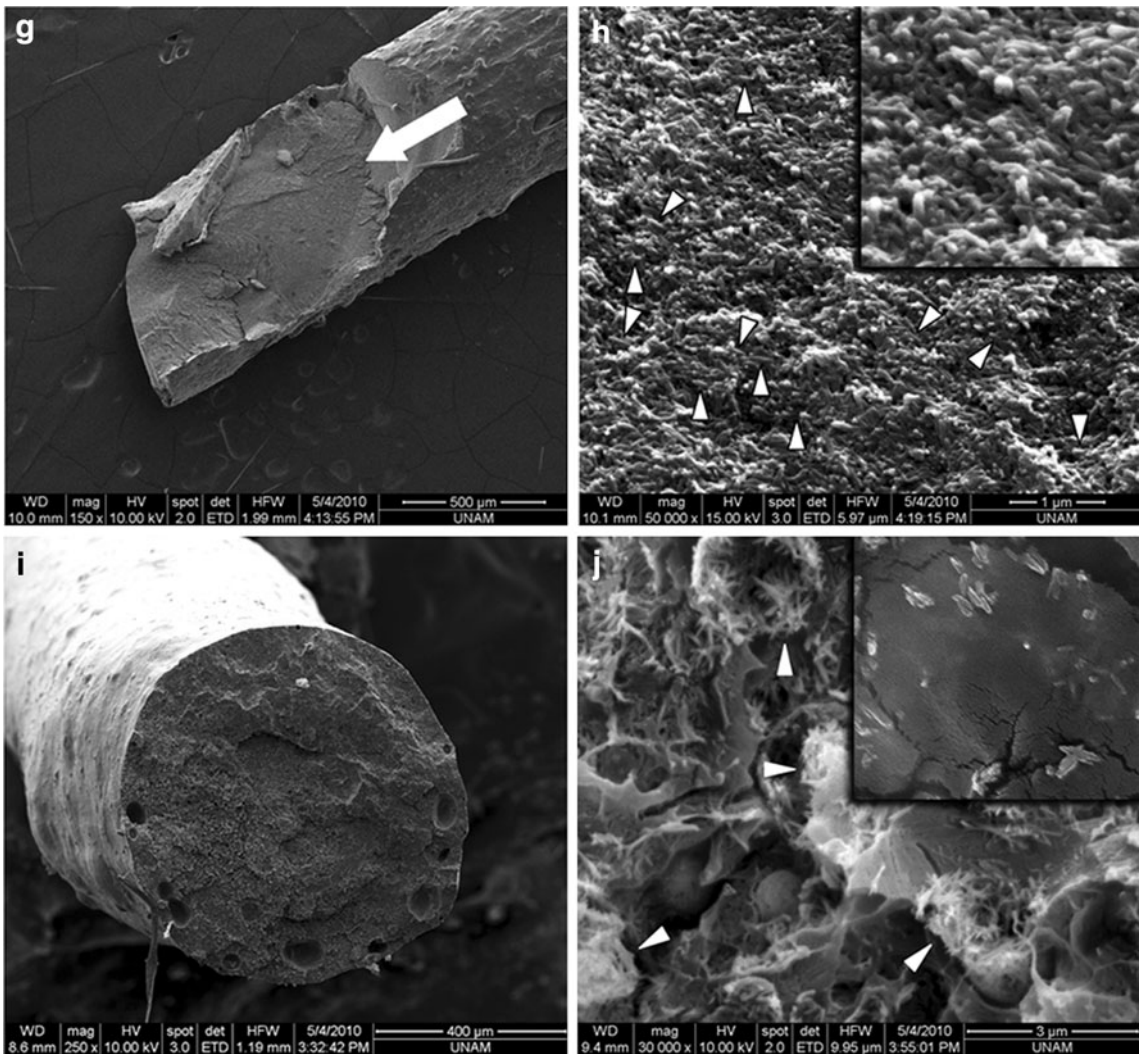

Fig. 3 continued

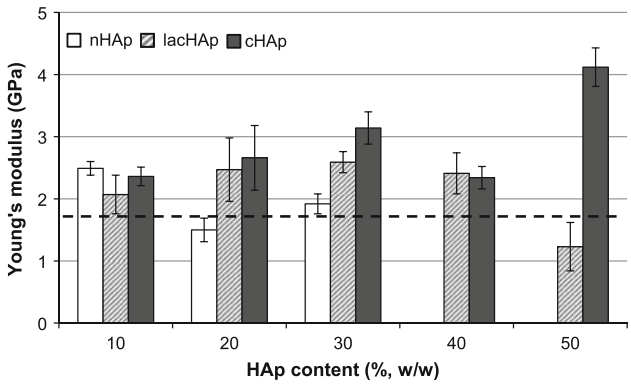

Fig. 4 Young's Modulus (tensile) values of PLLA–HAp composite fibers prepared with capillary rheometer. Values are expressed as means ± standard deviation. *Dashed line* represents YM value of pure PLLA fiber (1.75 GPa). Values for 40 and 50% nHAp containing composites could not be determined due to high brittleness

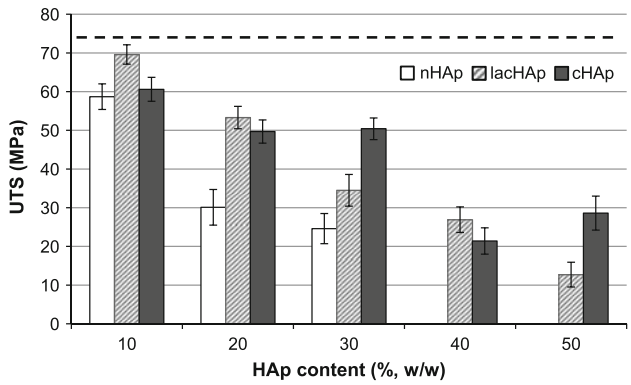

Fig. 5 UTS values of PLLA–HAp composite fibers prepared with capillary rheometer. Values are expressed as means ± standard deviation. *Dashed line* represents UTS value of pure PLLA fiber (73.9 MPa). Values for 40 and 50% nHAp containing composites could not be determined due to high brittleness

in this study and PLLA fibers loaded with HAp nanorods were devoid of the associated beneficiary effects on the ultimate tensile properties.

Increasing the commercial HAp (cHAp) loading in the composite fibers resulted in a steady increase or decrease in the YM or UTS values, respectively. Although these trends in YM and UTS were obeyed by the fibers in all cHAp ratios, 40% cHAp loading showed an irregular pattern. One possible explanation is that this is due to the large number of voids distributed randomly within matrix of cHAp loaded fibers (Fig. 3c), causing discontinuity in material throughout c-axis and causing premature failure during mechanical testing. Although such voids were observed in fibers with all cHAp loading ratios, the random nature of their distribution within the matrix has certainly some effect on such unexpected mechanical behaviors.

The UTS and YM values (73.9 MPa and 1.75 GPa, respectively) of the pure PLLA fibers obtained in this study were comparable or better than others reported in the literature for extruded pure polymers. For example, Weir et al. [43] produced PLLA (Resomer L210) rods of 2 mm diameter with extrusion and followed by annealing. The resulting rods had UTS of 64.3 MPa and YM of 0.67 GPa. Lewitus et al. [44] produced 0.1 mm thick PLLA films by extrusion and reported UTS of 57 MPa and YM of 1.79 GPa.

In Fig. 6, UTS and YM values were plotted against the composite's lacHAp nanorod content (up to 34%) and opposite trends are observed between these two. Increasing the proportion of any type of HAp in the composites had decreased the UTS values. This was expected since the presence of HAp particles between the polymer macromolecules decreases the polymer's crystallinity, and therefore, its mechanical strength. In general, presence of fillers decreases mechanical strength [45] and this is also valid in this study. Also, discontinuities in the matrix which were introduced by the added nanoparticles have a negative effect on the mechanical properties of the composite fibers. Although their association with the PLLA matrix was increased by chemically surface grafting them with lactic acid, the nanoparticles were still not bonded to matrix and act like defects.

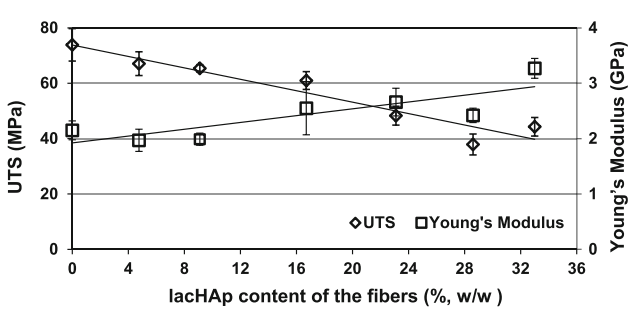

Fig. 6 UTS and Young's Modulus values of the lacHAp–PLLA composite fibers. Values are expressed as means ± standard deviation

3.6 Compressive properties of bone plates reinforced with PLLA–HAp composite fibers

Compressive properties of the composite fibers were expected to increase with the increasing HAp content within the structure (until reaching an optimum) because HAp nanorods, as would be expected for ceramic materials, cannot be deformed at level of compressive forces causing deformation of the polymers. Furthermore, longitudinally aligned HAp nanorods would be expected to resist compression much better than a continuous fiber reinforcement with the same material, due to elimination of crack propagation, as suggested by Ji and Gao [25]. It was not possible to directly experiment these hypotheses due to the fact that the produced composite fibers had small diameters and they failed through bending during compressive tests. Instead, bone plates reinforced with these composite fibers (Fig. 7) were compression tested through the long axes of both bone plates and the reinforcing fibers.

The compressive mechanical properties of these plates are presented in Table 1 where it is seen that incorporation of composite rods only marginally affect the YM values, the highest increase (ca. 1.31 GPa, a 4% increase) was observed with the plates containing 16 of the nHAp–PLLA composite fibers. The changes were small probably due to the low content of composite fibers in the final plates in which the mass of the each fiber constituted only 1% of the total mass of the plates. Reinforcement with nHAp containing fibers did not decrease the compressive strengths of the plates at all. Thus, the mechanical contribution of

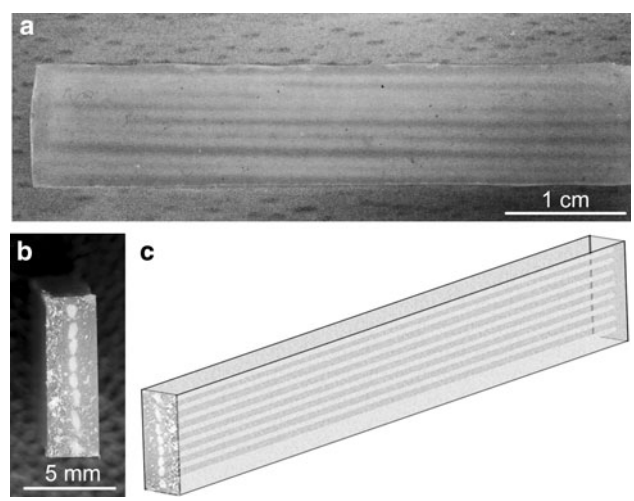

Fig. 7 PLLA bone plate reinforced with 8 PLLA-HAp composite fibers. **a** Top view, (**b**) Vertical cross section, (**c**) Schematical representation

Table 1 Compressive mechanical properties of PLLA bone plates reinforced with PLLA–HAp composite fibers

Reinforcement	Young's modulus (GPa)			Compressive strength (MPa)		
	No fiber	8 fibers	16 fibers	No fiber	8 fibers	16 fibers
No reinforcement	1.26 ± 0.04	–	–	109.8 ± 6.1	–	–
30% cHAp–PLLA fibers	–	1.25 ± 0.07	1.08 ± 0.11	–	100.0 ± 15.6	109.1 ± 6.9
30% nHAp–PLLA fibers	–	1.30 ± 0.03	1.31 ± 0.05	–	108.6 ± 3.4	110.3 ± 6.6
30% lacHAp–PLLA fibers	–	1.23 ± 0.06	1.21 ± 0.04	–	63.1 ± 14.4	76.4 ± 18.0

reinforcement fibers plates can be enhanced by increasing the volume fraction of the fibers within the plates both by optimizing the implant geometry and further compacting the fiber diameters through changing capillary rheometer process parameters.

In contrast to the positive effects of lacHAp on the tensile properties of the composite fibers, incorporation of lacHAp–PLLA composite fibers into the plates decreased the compressive strength significantly (from ca. 109.8 MPa to ca. 63.1 MPa with 8 fibers and to ca. 76.4 MPa with 16 fibers). This seemed to be in agreement with the observation that the surfaces of 30% or higher rations of lacHAp containing composite fibers were somewhat loose. Indeed, during compressive testing, the plates were observed to delaminate significantly, in parallel to the long axis, starting from the point where the plate makes a contact with the mechanical tester's clamps. Such a delamination did not occur in the case of composites containing other types of HAps; their failures occurred suddenly at the contact point with the tester's clamp.

As was mentioned in Sect. 3.4, the nanoparticles showed a high tendency of self-aggregation in composite fibers loaded with 30% or more lacHAp. This prevented their homogeneous distribution within the body of the composite fibers. Furthermore, it was concluded that these particles were localized at the surface of the fibers because they presented a surface with loosely attached particles. Therefore, at high lacHAp loadings the loose surface particles prevented strong integration of fibers with the matrix of the bone plates during molding. During compressive testing, plates impregnated with those fibers experienced delamination right at the fiber-matrix interfaces.

Plates reinforced with cHAp containing fibers showed some ambiguous results; plates with 8 fibers showed no change in YM values but a decrease in compressive strength, while the 16 fiber plates had a lower YM but no decrease in compressive strength. Overall, however, plates reinforced with nHAp containing fibers had higher or equal mechanical properties compared to the unreinforced plates.

Among all the tested HAp–reinforced fibers, the ones containing nHAp showed the best compressive performance. The compressive strengths of the plates reinforced with nHAp containing fibers are in agreement with those reported in the literature. Verheyen et al. [14] prepared PLLA–HAp composites containing 10 to 50% (w/w) sintered HAp particles (<45 μm) by an in situ polymerization technique and found that the compressive strength values were between 77.7 and 136.6 MPa. The YM values were about 4 times higher than ours (4.8 to 6.8 GPa). This difference between their and our results can be explained by the superiority of the in situ polymerization techniques in which monomers are polymerized in the presence of HAp particles, trapping them among entangled polymer chains. Also, unlike the rectangular prism shaped test samples used in this study, they used cylindrical test samples and this probably affected the results. However, their unloaded polymeric samples also had a much higher compressive modulus (5.1 GPa) than this study (1.26 GPa), so the data obtained in both studies could be considered comparable. Another composite produced in a different geometry (1 cm × 1 cm × 1 cm cubes) were obtained by Ignjatovic et al. [16] who compacted porous composites of PLLA and 20% (w/w) HAp nanoparticles with melt pressing and obtained a YM of 9.7 GPa and a compressive strength of 127 MPa. Since our experimental design aimed at producing reinforced bone plates containing HAp nanorods we could not employ machining or further processing. Even though their results are better, the comparison is not really valid. Huttunen et al. [34] prepared flat plates for hard tissue implants by melt pressing laminates from poly(L,DL-lactide) 70:30 loaded with (up to 50%, w/w) 50–125 μm β-tricalcium phosphate (β-TCP) granules where the individual layers were, beforehand, threaded inside a circular braid knitted from poly(L,D-lactide) 96:4 fibers. Compared to the unloaded samples with compressive yield strength of 97 MPa, β-TCP loading caused a decrease (to as low as 83 MPa) or increase (to as high as 123 MPa) in the compressive yield strength when the samples were tested parallel or perpendicular, respectively, to the sheet structure. Authors stated that fiber reinforcement did not have any significant effect on the compressive strength and modulus data were not supplied.

3.7 In situ degradation of PLLA–HAp composite fibers

3.7.1 Change in pH

The changes in the pH of ultrapure water during 42 days of in situ degradation are shown in Fig. 8. The initial pH of

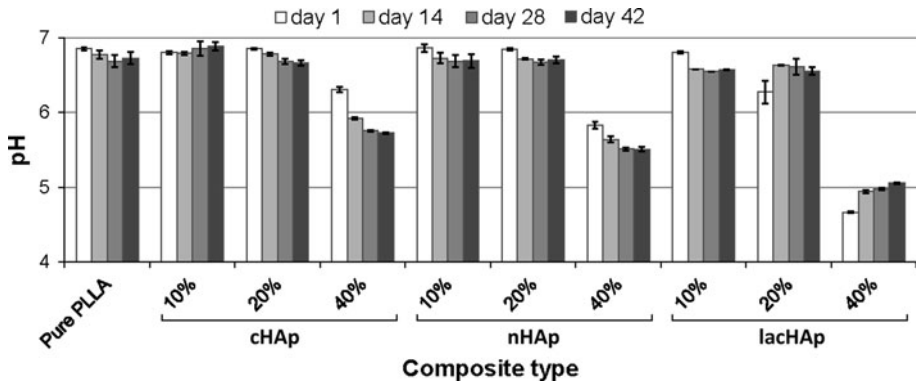

Fig. 8 pH of composite fibers during 42 days of in situ degradation in ultrapure water at 37°C

ultrapure water was 6.9 and there were detectable decreases in this value as the soluble oligomers leached out of the degrading polymer, increasing the number of acidic molecules in the medium. Composite fibers with 40% (w/w) HAp content of any type showed the most significant decrease in pH. HAp crystals are hydrophilic in nature and absorb water. In a polymer–HAp composite, HAp crystals within the polymer structure speed up transport of water from the surrounding medium into the composite bulk (unlike that observed in a hydrophobic polymeric material), increasing the degradation rate of polymer due to hydrolytic attack. Therefore, the observation that highest pH decrease is in the composites with the highest HAp (40%, w/w) should be a result of this water drawing activity of HAp into the polymer bulk, causing more hydrolysis in the polymer backbone. Although the interaction between HAp particles and the polymer matrix can further decreased due to water ingress (being the reason for the generally observed early loss of mechanical properties in in situ or in vivo), this situation is not expected to have an extensive effect on decrease of the pH of incubation medium.

3.7.2 Weight loss

Random hydrolytic scission is the main degradation route for PLLA and pH is also an important factor influencing the rate of degradation. Therefore, PBS was chosen as a basic buffered medium that is frequently used in the literature, instead of a simulated body fluid the components of which would not be expected to affect the degradation mechanism.

Weight losses (percent loss of the original weight) of pure PLLA or composite fibers were monitored in 0.1 M PBS for 42 days, to study the extent of degradation of the composite fibers developed in this study. As expected, the weight losses increased with increasing incubation duration for composites with HAp of any type (Fig. 9). Pure PLLA fibers and composite fibers containing only 10% (w/w) HAp of all types did not show a significant weight loss during the whole test duration. This was observed to a limited extent for the composite fibers with 20% (w/w) HAp of any sort. Although there is significant weight loss in composite fibers containing 40% (w/w) of all types of HAp, the most distinct weight loss was seen in composite fibers with 40% (w/w) lacHAp. This is in accordance with the most significant pH decrease observed with this composite type. Therefore, presence of higher amounts of HAp within composites facilitates the degradation, leads to weight loss and pH decrease. Also, lactic acid grafting of the HAp nanorods appears to speed up the degradation process further because the release of lactic acid from the HAp surfaces obviously increases the mediums acidity and PLLA degradation occurs faster in acidic media. It was noticed that the composite fibers containing 40% (w/w) lacHAp nanorods crumbled easily. No such behavior was observed with any other composite fibers.

The fibers were found to degrade with time in situ, therefore, it is expected that the mechanical properties of the implants that were reinforced with the here presented composite fibers will start to gradually lose their mechanical properties as soon as tissue fluids get in touch with the fibers. Since these reinforcing fibers are devised to be impregnated into the implants, however, the reach of tissue fluids to the fibers would not occur until the outer polymer matrix of the implant gets eroded or becomes leaky to the fluids. This can also prevent the rapid reach of tissue fluids to the filler–matrix interfaces, which otherwise cause early drop in the mechanical properties of the composite materials. Therefore, the time taken by the fluid to reach the reinforcing fibers can be tuned by changing the thickness of surrounding polymer matrix so that course of mechanical deterioration of the implants can be matched to bone healing.

3.8 In vitro evaluation of composite fibers

Even though the composite fibers were buried within the plates produced in this study, the surrounding PLLA matrix degrades and eventually the fibers embedded in the plates come in contact with the surrounding medium and with the

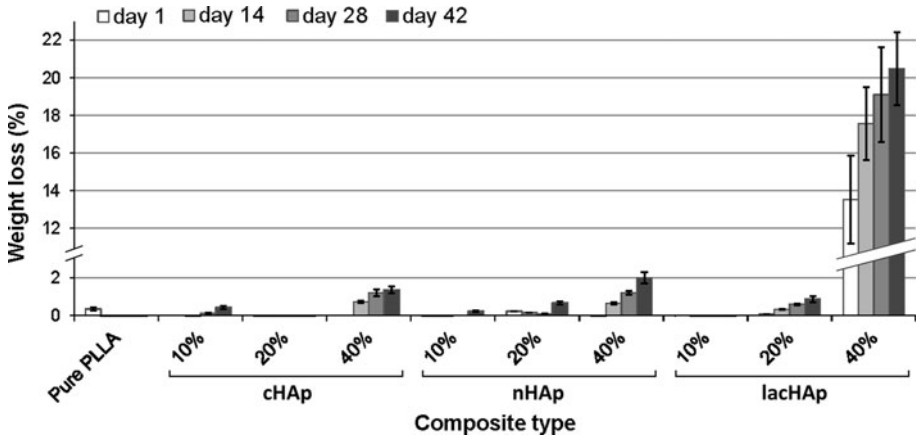

Fig. 9 Weight loss (%) of composite fibers during 42 days of in situ degradation in PBS at 37°C

cells. Furthermore, the degradation mechanism for PLLA is bulk erosion and this is expected to create gaps or voids within the plate structure, enabling the cells to penetrate inside the plate much earlier than the whole surrounding PLLA is degraded via surface erosion. This latter phenomenon could be realized sooner in the case of an implant device in which the buried composite fibers are close to the surface of the plate/device due to increased volume fraction of the fibers. Therefore, it was necessary to assess the interaction between the cells and the composite fibers.

Suitability of the produced composite fibers for use as a biocompatible implant was evaluated using rat bone marrow mesenchymal stem cells (MSC). During 14 days of incubation, MSC proliferation was monitored on sheet constructs consisting of fibers attached to each other, side by side, by spraying chloroform on PLLA or PLLA–HAp composite fibers. The cell numbers increased from Day 7 to Day 14 on all the construct types (Fig. 10). Despite the fact that the least cell number increase was observed on the constructs produced from pure PLLA fibers (slightly lower than 20%) this is still in agreement with the literature that polymers belonging to the PLA family do support osteoblast proliferation [46].

In all the other composite constructs, there were various types of HAp within the structure and all of these shoved a minimum 2-fold increase in cell numbers from day 7 to 14. The increase was not proportional with the HAp content in the constructs; presence of HAp seemed to be enough to enhance cell growth. Again, this is in agreement with the literature where the presence of HAp particles on the material surfaces provides highly favorable bone attachment sites for the tissue cells [19]. All the constructs were favorable for attachment of osteoblasts, which is an advantage in terms of attraction of these cells to the injury site whenever the bone is fixed with a bone plate made of the materials studied in this work.

It should be mentioned that the sheets of fibers (attached through solvent spray) were not impermeable and some of

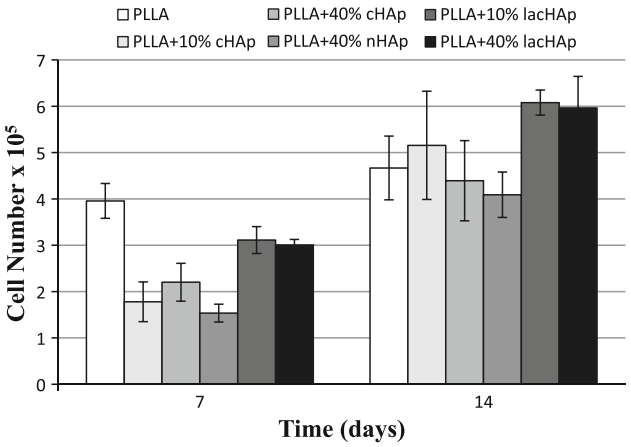

Fig. 10 MSC proliferation on PLLA–HAp constructs. Values are expressed as means ± standard deviation. All the increases in cell numbers within each series were statistically significant ($P < 0.05$), determined by unpaired two-tailed Student's *t*-test at a 95% confidence interval

the cells added on top of the sheets were lost through leakage. Therefore, the starting cell numbers on individual constructs were not constant. For example, cell numbers on lacHAp constructs was higher than the others, and this cannot be interpreted as a higher preference of cells for those constructs. Instead, this could probably be the result of the initial number of cells attached on these constructs was higher and this difference was maintained throughout the experiment. Nevertheless, all the increases in the cell numbers between days 7 and 14 within each series were statistically significant ($P < 0.05$).

In order to determine the cell behavior and to qualitatively monitor cell attachment and spreading on the constructs, samples were fixed 3 days after seeding, stained with FITC-labeled phalloidin and DAPI and observed with a confocal microscope (Fig. 11). It was observed that the cells attach well on the fiber surfaces of the scaffolds regardless of the fiber type, PLLA or PLLA–HAp

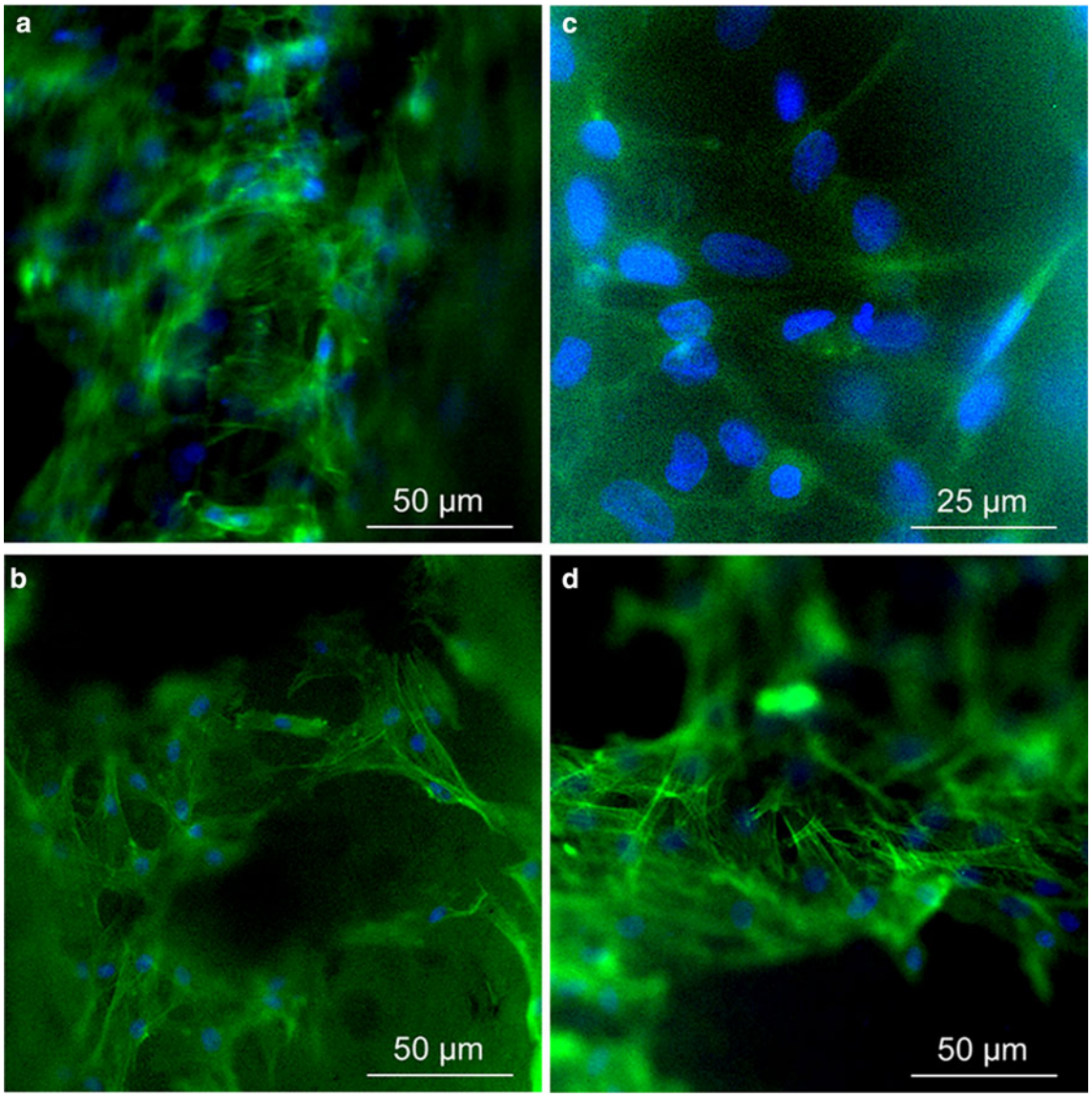

Fig. 11 BMSCs 3 days after seeding on bone plates. **a** PLLA, ×100, (**b**) PLLA–40% cHAp, ×100, (**c**) PLLA–40% nHAp, ×200, and (**d**) PLLA–40% lacHAp, ×100. FITC-phalloidin for cytoskeleton and DAPI for nucleus

composite fibers, as was shown by the elongated cytoskeletons on all types of fibers.

SEM micrographs revealed that cells spread well on composite fibers containing any type of HAp, in every polymer to HAp ratio tested (Fig. 12b–d). Especially in Fig. 12c, direct contact of cellular protrusions (filopodia) with higher chemical compatibility of the composite fiber is apparent. The nanorod-shaped HAp crystals are visible in the SEM (denoted as H) and their chemical identity was proven by EDX. In contrast to HAp containing composite fibers, both spread and normal cells were observed on HAp-free PLLA fiber (Fig. 12a). This is in agreement with the cell proliferation studies which showed the lowest proliferation with cells seeded on HAp-free PLLA fibers. Therefore, SEM and fluorescence microscopy results collectively suggest that nanocomposite fibers produced from PLLA and different HAp's in this study very well support osteoblast attachment, growth, and spreading, where the extent of these are higher in composites containing any type of HAp.

4 Conclusions

Reinforcement with composite polymer fibers containing aligned nHAp nanorods seemed to have a potential in increasing the compressive mechanical properties of bone plates or other hard tissue fixation implants, provided that quality and number of reinforcing fibers are increased. Alignment of the HAp nanorods towards the fiber axis can

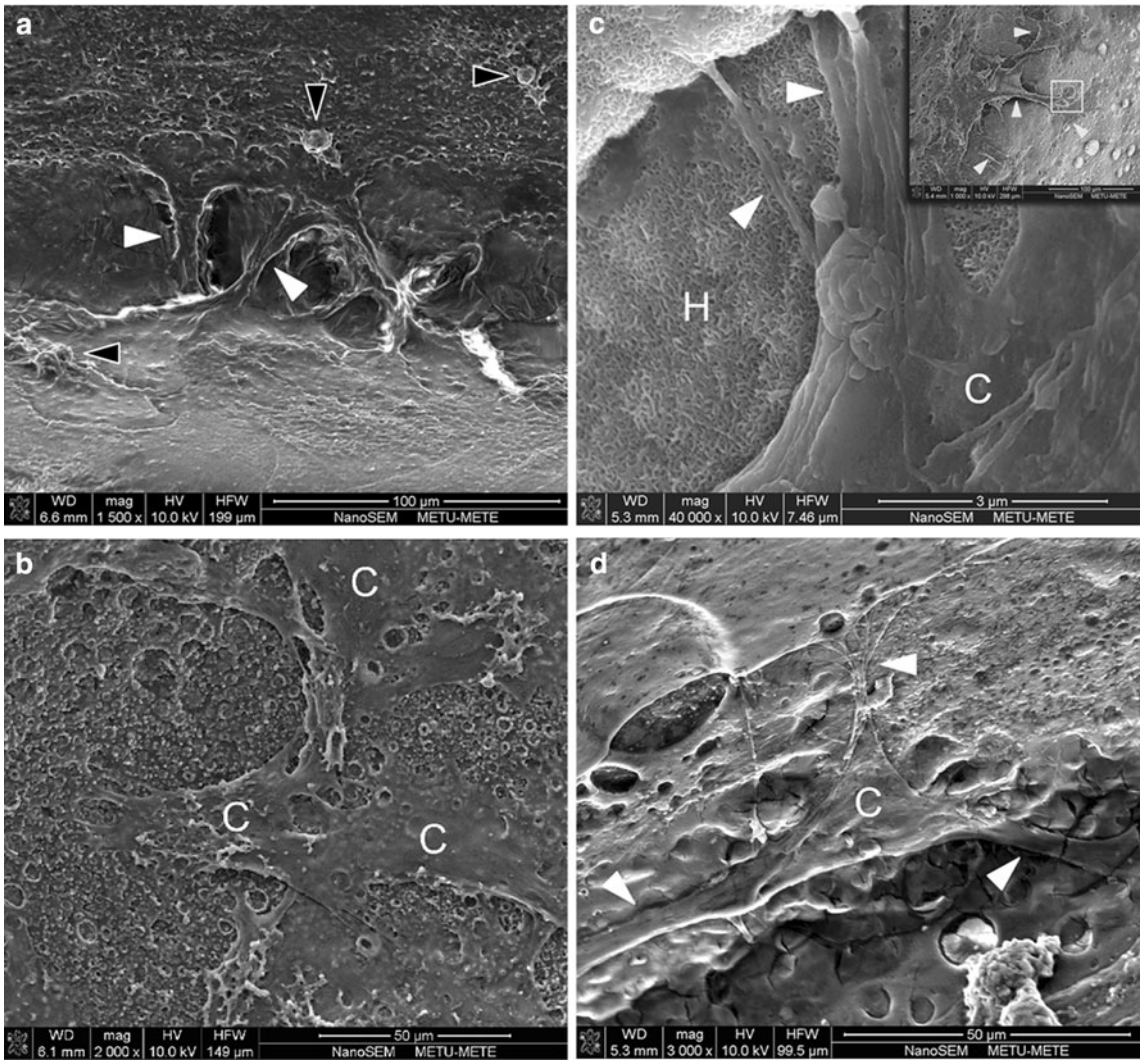

Fig. 12 SEM micrographs of cells on PLLA or PLLA–HAp composite fibers after 3 days of seeding. *White arrowheads* show protrusions of well-spread cells and *black arrowheads* show unspread cells; C: cells; H: HAp nanorods. **a** PLLA, ×1,500; (**b**) 10% cHAp–PLLA, ×2,000; (**c**) 10%nHAp–PLLA, ×40,000 (*inset*: same region at ×1,500; *white square* shows the magnified portion in **c**); (**d**) 10% lacHAp–PLLA, ×3,000

easily be achieved by a simple extrusion technique. Presence of HAp is definitely an asset but the optimum geometry and chemistry must be further studied.

Acknowledgments We gratefully acknowledge the support by the Scientific and Technical Research Council of Turkey (TUBITAK) (TBAG 105T508) and METU BAP.

References

1. Choueka J, Charvet JL, Alexander H, Oh YH, Joseph G, Blumenthal NC, Lacourse WC. Effect of annealing temperature on the degradation of reinforcing fibers for absorbable implants. J Biomed Mater Res. 1995;29:1309–15.
2. Benli S, Aksoy S, Havitcioglu H, Kucuk M. Evaluation of bone plate with low-stiffness material in terms of stress distribution. J Biomech. 2008;41(15):3229–35.
3. Fouad H. Effects of the bone-plate material and the presence of a gap between the fractured bone and plate on the predicted stresses at the fractured bone. Med Eng Phys. 2010;32:783–9.
4. Davis JR. Handbook of materials for medical devices. Metals Park, Ohio: ASM International; 2003. p. 17.
5. Sun ZL, Wataha JC, Hanks CT. Effects of metal ions on osteoblast-like cell metabolism and differentiation. J Biomed Mater Res. 1997;34:29–37.
6. Urban RM, Tomlinson MJ, Hall DJ, Jacobs JJ. Accumulation in liver and spleen of metal particles generated at nonbearing surfaces in hip arthroplasty. J Arthroplasty. 2004;19(8):94–101.
7. Kulkarni RK, Pani KC, Neuman C, Leonard F. Polylactic acid for surgical implants. Arch Surg. 1966;93:839–43.
8. Eppley BL. A bioabsorbable poly-L-lactide miniplate and screw system for osteosynthesis in oral and maxillofacial surgery—discussion. J Oral Maxillofac Surg. 1997;55(9):945–6.
9. Habal MB, Pietrzak WS. Key points in the fixation of the craniofacial skeleton with absorbable biomaterial. J Craniofac Surg. 1999;10(6):491–9.

10. Middleton JC, Tipton AJ. Synthetic biodegradable polymers as orthopedic devices. Biomaterials. 2000;21(23):2335–46.
11. Suzuki T, Kawamura H, Kasahara T, Nagasaka H. Resorbable poly-L-lactide plates and screws for the treatment of mandibular condylar process fractures: a clinical and radiologic follow-up study. J Oral Maxil Surg. 2004;62(8):919–24.
12. Bergsma JE, Rozema FR, Bos RRM, Boering G, de Bruijn WC, Pennings AJ. In vivo degradation and biocompatibility study of in vitro pre-degraded as-polymerized polylactide particles. Biomaterials. 1995;16(4):267–74.
13. Pruitt L, Furmanski J. Polymeric biomaterials for load-bearing medical devices. JOM. 2009;61(9):14–20.
14. Verheyen CCPM, De Wijn JR, Van Blitterswijk CA, De Groot D. Evaluation of hydroxylapatite/poly (L-lactide) composites: mechanical behavior. J Biomed Mater Res. 1992;26:1277–96.
15. Shikinami Y, Okuno M. Bioresorbable devices made of forged-composites of hydroxyapatite (HA) particles/poly L-lactide (PLLA). I. Basic characteristics. Biomaterials. 1999;20:859–77.
16. Ignjatovic N, Suljovrujic E, Budinski-Simendic J, Krakovsky I, Uskokovic D. Evaluation of hot-pressed hydroxyapatite/poly-L-lactide composite biomaterial characteristics. J Biomed Mater Res B. 2004;71B:284–94.
17. Rizzi SC, Heath DJ, Coombes AGA, Bock N, Textor M, Downes S. Biodegradable polymer/hydroxyapatite composites: surface analysis and initial attachment of human osteoblasts. J Biomed Mater Res. 2001;55:475–86.
18. Dalton JE, Cook SD, Thomas KA, Kay JF. The effect of operative fit and hydroxyapatite coating on the mechanical and biological response to porous implants. J Bone Joint Surg Am. 1995;77:97.
19. Ducheyne P, Qiu Q. Bioactive ceramics: the effect of surface reactivity on bone formation and bone cell function. Biomaterials. 1999;20:2287–303.
20. Furukawa T, Matsusue Y, Yasunaga T, Shikinami Y, Okuno M, Nakamura T. Biodegradation behavior of ultra-high-strength hydroxyapatite/poly (L-lactide) composite rods for internal fixation of bone fractures. Biomaterials. 2000;21:889–98.
21. Soballe K, Hansen ES, Brockstedt-Rasmussen H, Bünger C. Hydroxyapatite coating converts fibrous anchorage to bony fixation during continuous implant loading. J Bone Joint Surg. 1993;73:270.
22. Jarcho M, Kay JE, Gumaer KI, Doremus RH, Drobeck HP. Tissue, cellular and subcellular events at a bone-ceramic hydroxyapatite interface. J Bioeng. 1977;1:79–92.
23. Skrtic D, Antonucci JM, Eanes ED. Amorphous calcium phosphate-based bioactive polymeric composites for mineralized tissue regeneration. J Res Natl Inst Stand Technol. 2003;108: 167–82.
24. Van Blitterswijk CA, Grote JJ, Kuypers W, Blok-van Hoek CJG, Daems WTh. Biointeractions at the tissue/hydroxyapatite interface. Biomaterials. 1985;43:243–51.
25. Ji B, Gao H. Mechanical properties of nanostructure of biological materials. J Mech Phys Solids. 2004;52:1963–70.
26. Deng X, Hao J, Wang C. Preparation and mechanical properties of nanocomposites of poly(D,L-lactide) with Ca-defiient hydroxyapatite nanocrystals. Biomaterials. 2001;22:2867–73.
27. Kasuga T, Ota Y, Nogami M, Abe Y. Preparation and mechanical properties of polylactic acid composites containing hydroxyapatite fibers. Biomaterials. 2001;22(1):19–23.
28. Deng C, Weng J, Lu X, Zhou ZB, Wan JX, Qu SX, et al. Preparation and in vitro bioactivity of poly(D,L-lactide) composite containing hydroxyapatite nanocrystals. Mater Sci Eng C. 2008;28(8):1304–10.
29. Zheng X, Zhou S, Xiao Y, Yu X, Feng B. In situ preparation and characterization of a novel gelatin/poly(D,L-lactide)/hydroxyapatite nanocomposite. J Biomed Mater Res Part B. 2009;91B: 181–90.
30. Takayama T, Todo M, Takano A. The effect of bimodal distribution on the mechanical properties of hydroxyapatite particle filled poly(L-lactide) composites. J Mech Behav Biomed Mater. 2009;2(1):105–12.
31. Takayama T, Todo M. Improvement of mechanical properties of hydroxyapatite particle-filled poly(L-lactide) biocomposites using lysine tri-isocyanate. J Mater Sci. 2009;44:5017–20.
32. Xin F, Jian C, Jianming R, Zhongcheng Z, Jianpeng Z. Effects of surface modification on the properties of poly(lactide-co-glycolide) composite materials. Polym Plast Technol Eng. 2009;48: 658–64.
33. Suuronen R, Pohjonen T, Wessman L, Törmala P, Vainionpaa S. New generation biodegradable plate for fracture fixation. Comparison of bending strengths of mandibular osteotomies fixed with absorbable self-reinforced multi-layer poly-L-lactide plates and metallic plates. An experimental study in sheep. Clin Mater. 1992;9:77–84.
34. Huttunen M, Ashammakhi N, Törmälä P, Kellomäki M. Fibre reinforced bioresorbable composites for spinal surgery. Acta Biomater. 2006;2:575–87.
35. Parsons AJ, Ahmed I, Haque P, Fitzpatrick B, Niazi MIK, Walker GS, Rudd CD. Phosphate glass fibre composites for bone repair. J Bionic Eng. 2009;6:318–23.
36. Bühler M, Bourban PE, Manson JAE. Cellular composites based on continuous fibres and bioresorbable polymers. Compos A. 2008;39:1779–86.
37. Yubao L, De Wijn J, Klein CPAT, Van Der Meer S. Preparation and characterization of nanograde osteoapatite-like rod crystals. J Mater Sci Mater Med. 1995;5:252–5.
38. Qiu X, Hong Z, Hu J, Chen l, Chen X, Jing X. Hydroxyapatite surface modified by L-lactic acid and its subsequent grafting polymerization of L-lactide. Biomacromolecules. 2005;6:1193–9.
39. Kose GT, Kenar H, Hasirci N, Hasirci V. Macroporous poly (3-hydroxybutyrate-co-3-hydroxyvalerate) matrices for bone tissue engineering. Biomaterials. 2003;24(11):1949–58.
40. Cassanas G, Morssli M, Fabregue E, Bardet L. Vibrational spectra of lactic acid and lactates. J Raman Spectrosc. 1991; 22:409–13.
41. Hong Z, Zhang P, He C, Qiu X, Liu A, Chen L, et al. Nanocomposite of poly(L-lactide) and surface grafted hydroxyapatite: Mechanical properties and biocompatibility. Biomaterials. 2005;26(32):6296–304.
42. Cheang P, Khor KA. Effect of particulate morphology on the tensile behaviour of polymer–hydroxyapatite composites. Mat Sci Eng A. 2003;345(1–2):47–54.
43. Weir NA, Buchanan FJ, Orr JF, Dickson GR. Degradation of poly-L-lactide. Part 1: in vitro and in vivo physiological temperature degradation. Proc Inst Mech Eng H. 2004;218(5):307–19.
44. Lewitus D, McCarthy S, Ophir A, Kenig S. The effect of nanoclays on the properties of PLLA-modified polymers part 1: mechanical and thermal properties. J Polym Environ. 2006; 14:171–7.
45. Roeder RK, Converse GL, Kane RJ, Yue W. Hydroxyapatite-reinforced polymer biocomposites for synthetic bone substitutes. JOM. 2008;60(3):38–45.
46. Ishaug SL, Payne RG, Yaszemski MJ, Aufdemorte TB, Bizios R, Mikos AG. Osteoblast migration on poly(α-hydroxy esters). Biotechnol Bioeng. 1996;50:443–51.